
<https://doi.org/10.15407/ujpe68.4.219>

V.I. ROMANENKO,¹ N.V. KORNILOVSKA,² L.P. YATSENKO¹

¹Institute of Physics, Nat. Acad. of Sci. of Ukraine
(46, Nauky Ave., Kyiv 03028, Ukraine; e-mail: vr@iop.kiev.ua)

²Kherson National Technical University
(11, Instytuts'ka Str., Khmelnyts'kyi 29016, Ukraine)

LIGHT PRESSURE ON NANOPARTICLES IN THE FIELD OF COUNTER-PROPAGATING BICHROMATIC WAVES WITH AN ADDITIONAL RELAXATION CHANNEL FOR THE EXCITED-STATE POPULATION

Light pressure on nanoparticles containing impurity atoms or color centers interacting resonantly with the field has been considered. In the general case, the available crystalline environment of atoms prohibits the formation of a two-level interaction scheme of the atom or the color center with the field by eliminating the prohibition on some transitions with spontaneous radiation emission. As a result, some atoms remain temporarily in the states that do not interact with the laser radiation field, but relax in time to the ground state. A theory which enables the calculation of the light-pressure force on atoms or color centers (and, accordingly, on the nanoparticle, where they are located) and its dependence on the atom-field interaction parameters, as well as the relaxation parameters of the excited and intermediate states, has been developed. To analyze the influence of various factors on the light-pressure force, calculations are made for a model set of parameters and for the parameters corresponding to the interaction between triply charged erbium ions in erbium-doped Y₂SiO₅ crystals and color centers that emerge owing to the occupation of defects in diamond crystals by silicon atoms. It turned out that the color centers make it possible to reinforce the light pressure on small, much smaller than the light wavelength, nanoparticles by several orders of magnitude.

Keywords: atoms, nanoparticles, laser radiation, light pressure.

1. Introduction

The control over the motion of atoms and small particles with the help of laser radiation forms a basis

Citation: Romanenko V.I., Kornilovska N.V., Yatsenko L.P. Light pressure on nanoparticles in the field of the counter-propagating bichromatic waves with an additional relaxation channel for the excited state population. *Ukr. J. Phys.* **68**, No. 4, 219 (2023). <https://doi.org/10.15407/ujpe68.4.219>.
Цитування: Романенко В.І., Корніловська Н.В., Яценко Л.П. Світловий тиск на наночастинки у полі зустрічних біхроматичних хвиль з додатковим каналом релаксації населеності збудженого стану. *Укр. фіз. журн.* **68**, № 4, 219 (2023).

for the novel technologies aimed at manipulating biological objects [1, 2], as well as for new frequency standards [3, 4] and atomic gravimeters [5]. The manipulation of nanoobjects by means of laser radiation is performed via the light-pressure force.

In the simplest case of interaction between an atom and a monochromatic traveling wave, the radiation force can reach the value [6, 7]

$$F_{\text{rad}} = \frac{1}{2} \hbar k \gamma, \quad (1)$$

where γ is the rate of spontaneous emission by the atom in the excited state, $k = 2\pi/\lambda$, and λ

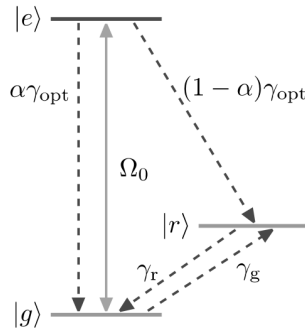


Fig. 1. Schematic diagram of the interaction between light and atoms that are resonant to laser radiation

is the laser radiation wavelength. This fundamental limit for the maximum light pressure on atoms located in the traveling-wave field can be exceeded, if the atom is subjected to the action of counter-propagating waves. In particular, this can be a sequence of counter-propagating light π -pulses [8], or counter-propagating bichromatic [9–14], frequency-modulated [15], or stochastic [16] waves, or counter-propagating waves of other types [14]. Besides the formation of the light-pressure force, counter-propagating waves can be used to hold atoms in a certain spatially confined region (in the atomic trap) [17–20].

The basis of the light-pressure action on atoms consists in the possibility of a cyclic interaction between the atoms and the field, when the spontaneous radiation emission by an atom in an excited state is accompanied by the transition of this atom into the ground state. This event becomes possible, because the selection rules prohibit transitions to other, non-working states. In the case where an atom is located in a crystalline environment, a lot of transitions that are forbidden for a free atom become allowed owing to the influence of the crystal-lattice field. As a result, the two-level scheme of the atom–field interaction becomes impossible. The transitions of the atom to states different from the ground and excited ones are followed in time by its return to the ground state.

Color centers in crystals interact with laser radiation in a similar way. They arise as a result of the electron capture by defects in the crystal lattice. In what follows, when considering the interaction of impurity atoms in crystals with the laser radiation field, we also mean the interaction of color centers with laser radiation. Below, both impurity atoms and color cen-

ters will be called “active atoms” due to the resonant character of their interaction with laser radiation.

The interaction of an active atom with the field in the presence of an additional relaxation channel can be approximately described by the three-level schematic diagram shown in Fig. 1. In the figure, $|e\rangle$ is an excited state of the active atom, $|g\rangle$ is its ground state, $|r\rangle$ is a set of states into which the atom can transit from the excited state after the spontaneous radiation emission, α is the probability of a transition into the $|g\rangle$ state after spontaneously emitting one photon, γ_{opt} is the rate of spontaneous emission from the excited state, γ_g and γ_r are constants describing the population relaxation in the states $|g\rangle$ and $|r\rangle$, and Ω_0 is the Rabi frequency, which is proportional to the intensity of the electric field created by laser radiation (it is responsible for the interaction of radiation with the atom). The atom is also characterized by one more parameter, which is not indicated in the figure: the coherence relaxation rate γ_{coh} (the non-diagonal element in the density matrix, which couples the states $|e\rangle$ and $|g\rangle$).

The transition frequencies of active atoms have to differ slightly from one another in order that all those atoms, if possible, interact resonantly with the field. Lanthanides, because of their possibility to transit between the states related to inner electronic shells whose energies are less dependent on the crystal environment, are obvious probable candidates for the study of the induced light pressure on solids with inclusions of active atoms. Another candidate for impurities in solids, which allow the light-pressure force to be significantly increased, is color centers. The influence of the crystalline environment in solids on their transition frequency is small because of the symmetry of their interaction with the crystalline environment. Examples of both variants – lanthanides and color centers – will be considered below.

The structure of the paper is as follows. The next Section contains basic equations. In Section 3, it is shown how the solution to the equations for the density matrix is constructed and how the light-pressure force on an atom (or a solid body containing this atom) in a monochromatic wave field is calculated in the framework of the three-level atom model. A theory of light pressure on a three-level atom in the field of counter-propagating bichromatic waves is developed in Section 4. In Section 5, the results of numerical calculations of the dependence of the light-

pressure force on some parameters describing the atom and its interaction with the field are presented, as well as the results of calculations of the force exerting by the light field of counter-propagating bichromatic waves on a Y_2SiO_5 crystal doped with erbium ions; here, erbium ions are “active atoms”. In addition, the light-pressure force on diamond nanoparticles with silicon impurities is also considered. The latter favor the formation of color centers with spectroscopic characteristics that provide a rather strong light-pressure force on the nanoparticles. The main conclusions of the work are given in Section 6.

2. Basic Equations

2.1. Electric field

Let the electric field strength created by two counter-propagating waves with the same carrier frequency ω at the point, where an atom is located in the nanoparticle, be described by the formula

$$\mathbf{E} = \mathbf{E}_1(t) \cos[\omega t - kz + \phi_1] + \mathbf{E}_2(t) \cos[\omega t + kz + \phi_2]. \quad (2)$$

Here, \mathbf{E}_1 and \mathbf{E}_2 are the time-dependent (in the general case) amplitudes of the field strengths of the counter-propagating waves, and ϕ_1 and ϕ_2 are the phases of those waves. The relation between the electric field at the atomic location point and the field beyond the nanoparticle depends on the nanoparticle shape. For example, the field strength E in a spherical nanoparticle whose size is small in comparison with the wavelength is coupled with the field E_{inc} in the medium via the formula [21]

$$E = \frac{3n_2}{n_1 + 2n_2} E_{\text{inc}}, \quad (3)$$

where n_1 is the refractive index of the nanoparticle material, and n_2 is the refractive index of the medium.

If there is only one monochromatic traveling wave, then $\mathbf{E}_2(t) = 0$, $\mathbf{E}_1(t) = \mathbf{E}_0$, and $\phi_1 = 0$ in Eq. (2) so that

$$\mathbf{E} = \mathbf{E}_0 \cos(\omega t - kz). \quad (4)$$

In the case of counter-propagating bichromatic waves, we have $\phi_1 = \phi_2 = 0$,

$$\begin{aligned} \mathbf{E}_1 &= \mathbf{E}_0 \cos\left(\delta t + \frac{1}{2}\varphi\right), \\ \mathbf{E}_2 &= \mathbf{E}_0 \cos\left(\delta t - \frac{1}{2}\varphi\right). \end{aligned} \quad (5)$$

The frequencies of the monochromatic components of bichromatic waves are equal to $\omega + \delta$ and $\omega - \delta$. The phase difference between the counter-propagating amplitude-modulated waves equals φ . The field acting on the atom looks like

$$\begin{aligned} \mathbf{E} &= \mathbf{E}_0 \cos(\omega t - kz) \cos\left(\delta t + \frac{1}{2}\varphi\right) + \\ &+ \mathbf{E}_0 \cos(\omega t + kz) \cos\left(\delta t - \frac{1}{2}\varphi\right). \end{aligned} \quad (6)$$

2.2. Equation for the density matrix

The equation for the density matrix, which describes doped atoms or color centers in nanoparticles, reads

$$i\hbar \frac{\partial}{\partial t} \varrho = [H, \varrho] + R, \quad (7)$$

where H is the Hamiltonian of the atom in the laser radiation field, and the term R describes the relaxation. In turn, the Hamiltonian has the form

$$H = \hbar\omega_a |e\rangle\langle e| + \hbar\omega_r |r\rangle\langle r| - \hat{\mathbf{d}} \mathbf{E}, \quad (8)$$

where ω_a is the frequency of atomic transition (the energy difference between the $|e\rangle$ and $|g\rangle$ states in Fig. 1), $\hbar\omega_r$ is the energy of the state $|r\rangle$, and $\hat{\mathbf{d}}$ is the dipole moment operator. In Eq. (8), the energy of the state $|g\rangle$ is assumed to equal zero, and the kinetic energy of the nanoparticle is not taken into account because of the large mass of the nanoparticle which the atom is connected with.

Let us introduce the detuning

$$\Delta = \omega_a - \omega \quad (9)$$

of the carrier frequencies of the counter-propagating waves from the frequency of the resonance transition in the atom and change from the basis of “bare” states $|g\rangle$, $|e\rangle$, $|r\rangle$ to the rotating basis

$$\begin{aligned} |\psi_g\rangle &= |g\rangle, \quad |\psi_e\rangle = e^{i(\omega_a - \Delta)t} |e\rangle, \\ |\psi_r\rangle &= e^{i(\omega_r - \Delta)t} |r\rangle. \end{aligned} \quad (10)$$

The density matrix in the basis of “bare” atomic states, ϱ , is expressed through the density matrix in the rotating basis, ρ , as follows:

$$\begin{aligned} \varrho_{gg} &= \rho_{gg}, \\ \varrho_{ee} &= \rho_{ee}, \\ \varrho_{ge} &= \rho_{ge} e^{i(\omega_a - \Delta)t}, \\ \varrho_{eg} &= \rho_{eg} e^{-i(\omega_a - \Delta)t}, \\ \varrho_{rr} &= \rho_{rr}. \end{aligned} \quad (11)$$

The transformations of the off-diagonal elements that include the state $|r\rangle$ are not given here, because they are not essential to our problem. Then, substituting Eqs. (8) and (11) into Eq. (7), we obtain

$$\begin{aligned} \frac{\partial \rho_{gg}}{\partial t} &= \frac{1}{2} i \rho_{ge} (\tilde{\Omega}_1^* + \tilde{\Omega}_2^*) - \frac{1}{2} i \rho_{eg} (\tilde{\Omega}_1 + \tilde{\Omega}_2) + \\ &+ \gamma_{\text{opt}} \alpha \rho_{ee} + \gamma_r \rho_{rr} - \gamma_g \rho_{gg}, \\ \frac{\partial \rho_{ge}}{\partial t} &= \frac{1}{2} i (\tilde{\Omega}_1 + \tilde{\Omega}_2) (\rho_{gg} - \rho_{ee}) + \\ &+ (i\Delta - \gamma_{\text{coh}}) \rho_{ge}, \end{aligned} \quad (12)$$

$$\begin{aligned} \frac{\partial \rho_{rr}}{\partial t} &= -\gamma_r \rho_{rr} + \gamma_g \rho_{gg} + \gamma_{\text{opt}} (1 - \alpha) \rho_{ee}, \\ \rho_{eg} &= \rho_{ge}^*, \quad \rho_{ee} = 1 - \rho_{gg} - \rho_{rr}. \end{aligned}$$

Here, the complex Rabi frequencies were introduced:

$$\tilde{\Omega}_1 = \Omega_1 e^{i\phi_1 - ikvt - ikz}, \quad \tilde{\Omega}_2 = \Omega_1 e^{i\phi_2 + ikvt + ikz}, \quad (13)$$

where z is the atom's coordinate at the time $t = 0$ in the laboratory reference frame, and v is the projection of the atom's velocity onto the z -axis. The atomic motion leads to the Doppler shift of the frequencies of the counter-propagating waves "seen" by the atom. The Rabi frequencies Ω_1 and Ω_2 are defined as follows:

$$\Omega_1 = -\frac{1}{\hbar} \mathbf{d}_{ge} \mathbf{E}_1, \quad \Omega_2 = -\frac{1}{\hbar} \mathbf{d}_{ge} \mathbf{E}_2. \quad (14)$$

In the absence of a laser field, Eqs. (12) give the equilibrium values for the populations of the states $|e\rangle$, $|g\rangle$, and $|r\rangle$:

$$\rho_{gg} = \frac{\gamma_r}{\gamma_r + \gamma_g}, \quad \rho_{rr} = \frac{\gamma_g}{\gamma_r + \gamma_g}, \quad \rho_{ee} = 0. \quad (15)$$

Note that the sum of the constants γ_r and γ_g gives the relaxation rate of the populations in the states $|e\rangle$ and $|g\rangle$ to equilibrium values (15), and their ratio is equal to the ratio between the equilibrium populations.

The constant γ_{coh} in Eqs. (12) is the relaxation rate of coherence ρ_{ge} . It is related to the constants γ_{opt} and γ_g via the relation

$$\gamma_{\text{coh}} = \frac{1}{2} \gamma_{\text{opt}} + \frac{1}{2} \gamma_g + \gamma_{\text{fl}}, \quad (16)$$

where the term γ_{fl} is associated with the influence of the environment on the growth of the coherence relaxation rate. The minimum coherence relaxation rate is obviously equal to $\frac{1}{2} \gamma_{\text{opt}} + \frac{1}{2} \gamma_g$.

When obtaining Eqs. (12), the rotating-wave approximation was used.

2.3. Light-pressure force acting on nanoparticles

The force of light pressure acting on a nanoparticle is obviously equal to the sum of the light-pressure forces acting on all active atoms in that nanoparticle. The force acting on an atom that is located in the nanoparticle and resonates with laser radiation is determined by the expression

$$\mathbf{F} = -\langle \nabla V \rangle, \quad (17)$$

where V is the Hamiltonian component responsible for the interaction of the atom with the field; in the dipole approximation, $V = -\mathbf{d}\mathbf{E}$. The angular brackets $\langle \dots \rangle$ denote the averaging over the atomic ensemble. It can also be said that expression (17) describes the force of light pressure acting on a mass that is equal to the mass per one atom in the nanoparticle that interacts in a resonance manner with the laser radiation field (the active atom).

Since only the off-diagonal elements of V differ from zero, the z -projection of the light-pressure force equals

$$F_z = -2 \text{Re} \rho_{eg} \frac{\partial V_{ge}}{\partial z}. \quad (18)$$

Expression (18) depends on both the coordinate and the time.

We consider the interaction of an active atom with the field in the reference frame coupled with the nanoparticle. For field (2), the expression for V_{ge} takes the form

$$\begin{aligned} V_{ge} &= \hbar \Omega_1(t) \cos[\omega t - kz - kvt + \phi_1(t)] + \\ &+ \hbar \Omega_2(t) \cos[\omega t + kz + kvt + \phi_2(t)], \end{aligned} \quad (19)$$

where Ω_1 and Ω_2 are determined by formulas (14).

After the atoms began to interact with the field, and some time τ_{qs} elapsed, a quasi-stationary solution to Eqs. (12) for the the density matrix is established. Then, the time-averaged value of the light-pressure force acting on one atom is equal to

$$\tilde{F}(z) = \frac{1}{T} \int_{\tau_{\text{qs}}}^{T+\tau_{\text{qs}}} F_z(z, t) dt, \quad (20)$$

where the time interval T is large as compared to $2\pi/\delta$. In so doing, we neglect the variation of the nanoparticle velocity during the time interval T .

After substituting Eq. (19) into Eq. (18) and taking Eq. (11) into account, in the rotating wave approximation, we have

$$F_z(z, t) = -\hbar k \operatorname{Im} \left(\rho_{eg} \tilde{\Omega}_1 - \rho_{eg} \tilde{\Omega}_2 \right). \quad (21)$$

Here, the complex Rabi frequencies are determined by equalities (13). Then, expression (21) for the interaction of the atom with the field of a monochromatic wave (4) takes the form

$$F_z(z, t) = -\hbar k \operatorname{Im} \left(\rho_{eg} \Omega_0 e^{-ikvt - ikz} \right), \quad (22)$$

where $\Omega_0 = -\frac{1}{\hbar} \mathbf{d}_{ge} \mathbf{E}_0$.

In the case where the atom interacts with counter-propagating bichromatic waves (6), expression (21) for $F(z, t)$ looks like

$$F_z(z, t) = -\hbar k \operatorname{Im} \left[\rho_{eg} \Omega_0 e^{-ikvt - ikz} \cos \left(\delta t + \frac{1}{2} \varphi \right) - \rho_{eg} \Omega_0 e^{ikvt + ikz} \cos \left(\delta t - \frac{1}{2} \varphi \right) \right]. \quad (23)$$

The light-pressure force averaged over the ensemble of atoms that are resonant to laser radiation is obtained by averaging Eq. (20) over the initial atomic coordinate in the laboratory reference frame,

$$\bar{F} = \frac{k}{2\pi} \int_0^{2\pi/k} \tilde{F}_z(z) dz, \quad (24)$$

3. Light-Pressure Force Acting on a Nanoparticle in the Field of Monochromatic Traveling Wave

For a monochromatic traveling wave, an analytic expression for the light-pressure force can be found. From Eqs. (12) and taking the definition of complex Rabi frequencies into account [see Eqs. (13)], we obtain the following equations for the quasi-stationary elements of the density matrix:

$$\begin{aligned} 0 &= \frac{1}{2} i \rho_{ge} \Omega_0 e^{ikvt + ikz} - \frac{1}{2} i \rho_{eg} \Omega_0 e^{-ikvt - ikz} + \\ &+ \gamma_{\text{opt}} \alpha \rho_{ee} + \gamma_r \rho_{rr} - \gamma_g \rho_{gg}, \\ 0 &= \frac{1}{2} i \Omega_0 e^{-ikvt - ikz} (\rho_{gg} - \rho_{ee}) + \\ &+ (i\Delta + kv - \gamma_{\text{coh}}) \rho_{ge}, \end{aligned} \quad (25)$$

$$0 = -\gamma_r \rho_{rr} + \gamma_g \rho_{gg} + \gamma_{\text{opt}} (1 - \alpha) \rho_{ee},$$

$$\rho_{eg} = \rho_{ge}^*, \quad \rho_{ee} = 1 - \rho_{gg} - \rho_{rr}.$$

The substitution of the solution to those equations into expression (22) for the force of light pressure in the field of a monochromatic traveling wave gives

$$\begin{aligned} F(z, t) &= \hbar k \Omega_0^2 \gamma_{\text{coh}} \gamma_r \gamma_{\text{opt}} \times \\ &\times \left[2(\Delta + kv)^2 (\gamma_r + \gamma_g) \gamma_{\text{opt}} + \right. \\ &+ \Omega_0^2 \gamma_{\text{coh}} (2\gamma_r + \gamma_g + (1 - \alpha) \gamma_{\text{opt}}) + \\ &\left. + 2\gamma_{\text{coh}}^2 (\gamma_g + \gamma_r) \gamma_{\text{opt}} \right]^{-1}. \end{aligned} \quad (26)$$

As one can see, the force of light pressure in the field of a monochromatic traveling wave does not depend on the time and the coordinate.

The populations of the excited, $n_e = \rho_{ee}$, and ground, $n_g = \rho_{gg}$, states equal

$$\begin{aligned} n_e &= \Omega_0^2 \gamma_{\text{coh}} \gamma_r \left[2(\Delta + kv)^2 (\gamma_r + \gamma_g) \gamma_{\text{opt}} + \right. \\ &+ \Omega_0^2 \gamma_{\text{coh}} (2\gamma_r + \gamma_g + (1 - \alpha) \gamma_{\text{opt}}) + \\ &\left. + 2\gamma_{\text{coh}}^2 (\gamma_g + \gamma_r) \gamma_{\text{opt}} \right]^{-1}, \\ n_g &= \gamma_r \left[2\gamma_{\text{coh}}^2 \gamma_{\text{opt}} + \gamma_{\text{coh}} \Omega_0^2 + \right. \\ &+ 2\gamma_{\text{opt}} (\Delta^2 + (kv)^2) \left. \right] \times \\ &\times \left[2(\Delta + kv)^2 (\gamma_r + \gamma_g) \gamma_{\text{opt}} + \right. \\ &+ \Omega_0^2 \gamma_{\text{coh}} (2\gamma_r + \gamma_g + (1 - \alpha) \gamma_{\text{opt}}) + \\ &\left. + 2\gamma_{\text{coh}}^2 (\gamma_g + \gamma_r) \gamma_{\text{opt}} \right]^{-1}. \end{aligned} \quad (27)$$

By comparing Eqs. (26) and (27), we see that

$$F(z, t) = \hbar k \gamma_{\text{opt}} n_e, \quad (28)$$

which is in total agreement with the elementary theory of light pressure [6].

If we put $\alpha = 1$ and $\gamma_g = 0$ (there are no $|r\rangle$ states) in Eq. (26), we obtain an expression for the light-pressure force in the two-level scheme of atom-field interaction [6]:

$$\begin{aligned} F(z, t) &= \frac{1}{2} \hbar k \Omega_0^2 \gamma_{\text{coh}} \gamma_{\text{opt}} \left[(\Delta + kv)^2 \gamma_{\text{opt}} + \right. \\ &\left. + \Omega_0^2 \gamma_{\text{coh}} + \gamma_{\text{coh}}^2 \gamma_{\text{opt}} \right]^{-1}. \end{aligned} \quad (29)$$

As the field intensity grows, the expressions obtained for the light-pressure force in the field of a monochromatic traveling wave reach the corresponding maximum values:

$$F_{\max} = \frac{\hbar k \gamma_{\text{opt}} \gamma_r}{[\gamma_{\text{opt}}(1 - \alpha) + 2\gamma_r + \gamma_g]} \quad (30)$$

for the three-level scheme of atom-field interaction and

$$F_{2\max} = \frac{\hbar k \gamma_{\text{opt}}}{2} \quad (31)$$

for the two-level one. It is easy to see that $F_{2\max} \geq F_{\max}$ for all time. The equality sign corresponds to the case $\alpha = 1$ and $\gamma_g = 0$, when the three-level system becomes a two-level one.

4. Light-Pressure Force Acting on a Nanoparticle in the Field of Counter-Propagating Bichromatic Waves

If the Doppler frequency shift is small, the solution to the equations for the density matrix (12) can be found in the form of a Fourier series. Bearing in mind that the ‘‘active’’ atoms comprise only a small fraction in the composition of the nanoparticle material, one may expect that the acceleration of nanoparticles – and, hence, the velocity that they be acquired, when interacting with the field – is low. An obvious criterion that the velocity is low is a small value of the Doppler shift in comparison with the spontaneous emission rate for the atom from the excited state, $kv < \gamma_{\text{opt}}$. For example, for $\lambda = 0.6$ nm and $\gamma_{\text{opt}}/(2\pi) = 10$ MHz, we have $v < 6$ m/s. Under optimal conditions for the atom-field interaction [12], the much weaker requirement $kv < \delta$ can be the criterion, since, in this case, the width of the maximum in the dependence of the light-pressure force on the atomic velocity for a two-level atom is somewhat smaller than $\delta/(2k)$.

The solution to Eqs. (12) for the density matrix in the case of low nanoparticle velocity can be presented in the form of the Fourier series,

$$\rho_{pq} = \sum_{n=-\infty}^{\infty} r_{pq,n} e^{in\delta t}, \quad (32)$$

where the subscripts p and q enumerate the atomic states. We should substitute Eq. (32) into the equations for the density matrix [Eq. (12)] and for the field

[Eq. (5)], and equate the terms on the right- and left-hand sides of the equations with the same multipliers $e^{in\delta t}$. As a result, we get

$$\begin{aligned} in\delta r_{gg,n} &= \frac{1}{4} i r_{ge,n-1} \Omega_0 \left(e^{ikz+\frac{1}{2}i\varphi} + e^{-ikz-\frac{1}{2}i\varphi} \right) + \\ &+ \frac{1}{4} i r_{ge,n+1} \Omega_0 \left(e^{ikz-\frac{1}{2}i\varphi} + e^{-ikz+\frac{1}{2}i\varphi} \right) - \\ &- \frac{1}{4} i r_{eg,n-1} \Omega_0 \left(e^{-ikz+\frac{1}{2}i\varphi} + e^{ikz-\frac{1}{2}i\varphi} \right) - \\ &- \frac{1}{4} i r_{eg,n+1} \Omega_0 \left(e^{-ikz-\frac{1}{2}i\varphi} + e^{ikz+\frac{1}{2}i\varphi} \right) + \\ &+ \gamma_{\text{opt}} \alpha r_{ee,n} + \gamma_r r_{rr,n} - \gamma_g r_{gg,n}, \\ in\delta r_{ge,n} &= -\frac{1}{4} i \Omega_0 \left(e^{-ikz+\frac{1}{2}i\varphi} + e^{ikz-\frac{1}{2}i\varphi} \right) w_{n-1} - \\ &- \frac{1}{4} i \Omega_0 \left(e^{-ikz-\frac{1}{2}i\varphi} + e^{ikz+\frac{1}{2}i\varphi} \right) w_{n+1} + \\ &+ (i\Delta - \gamma_{\text{coh}}) r_{ge,n}, \\ in\delta r_{rr,n} &= -\gamma_r r_{rr,n} + \gamma_g r_{gg,n} + \gamma_{\text{opt}}(1 - \alpha) r_{ee,n}. \\ r_{eg,n} &= r_{ge,-n}^*, \quad r_{ee,n} + r_{gg,n} + r_{rr,n} = \xi_n, \\ w_n &= r_{ee,n} - r_{gg,n}, \end{aligned} \quad (33)$$

Here, w_n is the Fourier component of the population inversion $\rho_{ee} - \rho_{gg} = w_n e^{in\delta t}$, and

$$\xi_n = \begin{cases} 1 & n = 0 \\ 0 & n \neq 0. \end{cases} \quad (34)$$

The time-averaged value of the light-pressure force (23) acting on an atom with the coordinate z in the nanoparticle is given by the expression

$$\begin{aligned} F_z(z) &= \hbar k \Omega_0 \text{Im} \left[-r_{eg,-1} e^{-ikz+i\varphi/2} - \right. \\ &- r_{eg,1} e^{-ikz-i\varphi/2} + \\ &\left. + r_{eg,-1} e^{ikz-i\varphi/2} + r_{eg,1} e^{ikz+i\varphi/2} \right]. \end{aligned} \quad (35)$$

To find the light-pressure force per one atom in the nanoparticle, we must solve Eq. (33), substitute the solution into Eq. (35), and further average the result over z . For this purpose, using Eq. (33), we determine $r_{rr,n}$, $r_{ee,n}$, and $r_{rr,n}$ as functions of w_n :

$$\begin{aligned} r_{gg,n} &= \frac{-(\gamma_{\text{opt}}(1 - \alpha) + i\delta n + \gamma_r)w_n}{2i\delta n + 2\gamma_r + \gamma_{\text{opt}}(1 - \alpha) + \gamma_g} + \\ &+ \frac{(\gamma_r + i\delta n)\xi_n}{2i\delta n + 2\gamma_r + \gamma_{\text{opt}}(1 - \alpha) + \gamma_g}, \\ r_{ee,n} &= \frac{(i\delta n + \gamma_g + \gamma_r)w_n + \xi_n(\gamma_r + i\delta n)}{2i\delta n + 2\gamma_r + \gamma_{\text{opt}}(1 - \alpha) + \gamma_g}, \\ r_{rr,n} &= \xi_n - r_{gg,n} - r_{ee,n} \end{aligned} \quad (36)$$

Then we substitute the expressions found for $r_{gg,n}$, $r_{ee,n}$, and $r_{rr,n}$ into Eqs. (33). As a result, these equations take the form

$$\begin{aligned} 0 &= \frac{1}{2}iar_{ge,n-1}\Omega_0 + \frac{1}{2}ibr_{ge,n+1}\Omega_0 - \\ &- \frac{1}{2}ibr_{eg,n-1}\Omega_0 - \frac{1}{2}iar_{eg,n+1}\Omega_0 + \\ &+ \Gamma_{1,n}w_n + \xi_n\Gamma_{0,n}, \\ in\delta r_{ge,n} &= -\frac{1}{2}i\Omega_0bw_{n-1} - \frac{1}{2}i\Omega_0aw_{n+1} + \\ &+ (i\Delta - \gamma_{\text{coh}})r_{ge,n}, \quad r_{eg,n} = r_{ge,-n}^*. \end{aligned} \quad (37)$$

Here, we introduced

$$a = \cos\left(kz + \frac{1}{2}\varphi\right), \quad b = \cos\left(kz - \frac{1}{2}\varphi\right) \quad (38)$$

and

$$\begin{aligned} \Gamma_{0,n} &= \frac{(i\alpha\gamma_{\text{opt}} - i\gamma_g - i\gamma_r + \delta n)\delta n + \gamma_r\gamma_{\text{opt}}}{2i\delta n + 2\gamma_r + \gamma_{\text{opt}}(1 - \alpha) + \gamma_g}, \\ \Gamma_{1,n} &= \frac{(\gamma_g + \gamma_r + i\delta n)(\gamma_{\text{opt}} + i\delta n)}{2i\delta n + 2\gamma_r + \gamma_{\text{opt}}(1 - \alpha) + \gamma_g}. \end{aligned} \quad (39)$$

The case with $\alpha = 1$ and $\gamma_g = 0$ corresponds to the two-level scheme of atom–field interaction.

To calculate the light-pressure force from Eqs. (37), we have to find $r_{eg,-1}$ and $r_{eg,+1}$, and substitute the obtained values into Eq. (35) with the subsequent averaging over z . We have

$$r_{ge,n} = -\frac{1}{2}\frac{\Omega_0(bw_{n-1} + aw_{n+1})}{-i\gamma_{\text{coh}} - \Delta + n\delta}, \quad (40)$$

which gives

$$r_{eg,n} = \frac{1}{2}\frac{\Omega_0(aw_{n-1} + bw_{n+1})}{-i\gamma_{\text{coh}} + \Delta + n\delta}. \quad (41)$$

Here, we account for that $w_{-n}^* = w_n$, because the population inversion is a real-valued quantity. Substituting expressions (40) and (41) into the first of Eqs. (37), we obtain

$$A_{n+2}w_{n+2} + B_nw_n + A_nw_{n-2} = D\xi_n, \quad (42)$$

where

$$\begin{aligned} A_n &= -\frac{iab\Omega_0^2}{2u_{n-1}v_{n-1}} [(n-1)\delta - i\gamma_{\text{coh}}], \\ B_n &= -\frac{i\Omega_0^2}{4} \left(\frac{a^2}{u_{n-1}} + \frac{b^2}{u_{n+1}} + \frac{a^2}{v_{n+1}} + \frac{b^2}{v_{n-1}} \right) + \end{aligned}$$

$$+ \frac{(n\delta - i\gamma_r - i\gamma_g)(-n\delta + i\gamma_{\text{opt}})}{2i\delta n + 2\gamma_r + \gamma_{\text{opt}}(1 - \alpha) + \gamma_g}, \quad (43)$$

$$D = -\frac{\gamma_r\gamma_{\text{opt}}}{\gamma_g + 2\gamma_r + (1 - \alpha)\gamma_{\text{opt}}}.$$

Here,

$$u_n = -\Delta - i\gamma_{\text{coh}} + n\delta, \quad v_n = \Delta - i\gamma_{\text{coh}} + n\delta. \quad (44)$$

By its form, the recurrence relation (42) for the Fourier components w_n of the population inversion coincides with a similar relation for the case of interaction between a two-level atom and counter-propagating bichromatic waves [9]. Let us solve it by reducing the three-term relation to a two-term one. Note that if $n > 0$, the right-hand side of Eq. (42) equals zero. All w_n with odd n also vanish. Let us introduce a set of ratios $\Pi_n = w_{n+2}/w_n$. As a result, Eq. (42), yields

$$w_n \left(A_{n+2}\Pi_n + B_n + \frac{A_n}{\Pi_{n-2}} \right) = 0. \quad (45)$$

This equation is valid for $n \geq 2$. From whence, we have the following binomial recurrence relation for Π_n :

$$\Pi_{n-2} = -\frac{A_n}{A_{n+2}\Pi_n + B_n}. \quad (46)$$

Putting $\Pi_n = 0$ for a sufficiently large n and using formula (46), we iteratively determine all Π_n down to Π_0 . Then, knowing at least one of the Fourier components of the population inversion and using the already known sequence of Π_n , we can find values for all required w_n .

Equation (42) for $n = 0$ looks like

$$A_2w_2 + B_0w_0 + A_0w_{-2} = D \quad (47)$$

and makes it possible to determine w_0 . Let us express w_{-2} and w_2 in terms of w_0 and Π_0 :

$$w_2 = \Pi_0w_0, \quad w_{-2} = w_2^* = \Pi_0^*w_0^* = \Pi_0^*w_0. \quad (48)$$

Substituting Eq. (48) into Eq. (47), we obtain

$$w_0 = \frac{D}{A_0^*\Pi_0 + B_0 + A_0\Pi_0^*}. \quad (49)$$

Here, we took into account that $A_2 = A_0^*$.

The time-averaged populations of the ground, $r_{gg,0}$, and excited, $r_{ee,0}$, states depend on the coordinate and are equal to

$$\begin{aligned} n_g &= \frac{\gamma_r - w_0 [(1 - \alpha)\gamma_{\text{opt}} + \gamma_r]}{(1 - \alpha)\gamma_{\text{opt}} + 2\gamma_r + \gamma_g}, \\ n_e &= \frac{(\gamma_r + \gamma_g)w_0 + \gamma_r}{(1 - \alpha)\gamma_{\text{opt}} + 2\gamma_r + \gamma_g}. \end{aligned} \quad (50)$$

To find the light-pressure force acting on an atom from Eq. (35), it is necessary to express the off-diagonal elements of the density matrix that are contained in this equation in terms of w_0 and Π_0 according to formula (41):

$$\begin{aligned} r_{eg,-1} &= \frac{1}{2}w_0 \frac{\Omega_0 (b + a\Pi_0^*)}{-i\gamma_{\text{coh}} + \Delta - \delta}, \\ r_{eg,1} &= \frac{1}{2}w_0 \frac{\Omega_0 (b\Pi_0 + a)}{-i\gamma_{\text{coh}} + \Delta + \delta}. \end{aligned} \quad (51)$$

To obtain the averaged force of light pressure acting on slow nanoparticles, we should average expression (35) for the light-pressure force:

$$\bar{F} = \frac{1}{\lambda} \int_0^\lambda F(z) dz. \quad (52)$$

Similarly, by averaging Eq. (50) over the coordinate, it is possible to find the populations in the ground and excited states, and, using the normalization condition, the population of the $|r\rangle$ state.

5. Results and Discussion

The light-pressure force has been studied in the framework of the two-level model of interaction between the atom and bichromatic waves for more than three decades [9–14], and the interest in it still remains high [22–24]. The aim of our research is to find how the model parameters associated with the presence of an additional level affect the light-pressure force. Another parameter that will be considered here and whose variation has not been analyzed earlier is the coherence relaxation rate γ_{coh} . As was shown above (see Section 2.2), its minimum value equals $\frac{1}{2}(\gamma_{\text{opt}} + \gamma_g)$.

In what follows, from the whole set of parameters of the problem, the attention will be focused on those that provide optimal conditions for the interaction of atoms with the field. It is known that a strong light-pressure force and, simultaneously, a large width of

the maximum in the light-pressure force dependence on the atomic velocity can be achieved at some combination of mutually related Ω_0 -, δ -, and φ -values. In work [12], the force of bichromatic light pressure was analyzed in the basis of “dressed” states in the framework of the Floquet approach. It was shown that this force emerges as a result of the Landau–Zener transitions between “dressed” states (the eigenstates of the Floquet Hamiltonian). Under the condition $\phi = \pi/4$ and, at the optimal Rabi frequency

$$\Omega_0 = \delta\sqrt{6}, \quad (53)$$

the force acting on an atom dwelling in one of the “dressed” states reaches a maximum value and equals

$$F_{\text{bichro}} = \frac{2\hbar k\delta}{\pi}. \quad (54)$$

In order to determine the average force acting on an atom, it is necessary to know the populations in the “dressed” Floquet states. It is important that those states are divided into two classes in which the atoms are subjected to the action of forces which have identical magnitudes, but opposite directions. As a result, the resulting force is less than the maximum force (54) and can be found only using numerical methods. In calculations [11–13], the obtained maximum values were half the value given by Eq. (54). This fact testifies that the populations of “dressed” states in the cited calculations were $\frac{3}{4}$ and $\frac{1}{4}$. These populations depend on the relaxation constants. Since it was taken that $\gamma_{\text{coh}} = \gamma_{\text{opt}}/2$ in the cited works, the relevant calculations almost always gave a pressure force value close to $\frac{1}{2}F_{\text{bichro}}$.

Below, the light-pressure force is calculated assuming condition (53). We compare the light-pressure force acting on nanoparticles in the field of counter-propagating bichromatic waves [Eq. (24)] with the maximum force of light pressure acting on nanoparticles in the field of a monochromatic traveling wave [Eq. (30)], as well as with F_{bichro} .

5.1. Examples of calculations for a parameter set

First of all, let us consider how the light-pressure force depends on the parameter α , which describes the ratio between the numbers of spontaneous transitions onto the lower working level $|g\rangle$ and the remaining levels $|r\rangle$, where the atoms do not directly interact

with the laser radiation field. The results of calculations obtained for various coherence relaxation rates are plotted in Fig. 2. As one can see, for the selected parameters of the atom–field interaction, the light-pressure force acting on a nanoparticle in the field of counter-propagating bichromatic waves can exceed the light-pressure force acting on a nanoparticle in the field of a monochromatic traveling wave by more than an order of magnitude. As α increases, the ratio \bar{F}/F_{\max} decreases. It should be noted that the light-pressure force magnitude (rather than the \bar{F}/F_{\max} ratio) increases a little with the growth of α . Figure 2 demonstrates the expected decrease of \bar{F}/F_{\max} with the increase of γ_{coh} , in total agreement with the fact that the induced light-pressure force observed in the field of counter-propagating light waves is a coherent phenomenon.

In Fig. 3, the α -dependences of the light-pressure forces acting on a nanoparticle at various values of the sum $\gamma_g + \gamma_r$ of the relaxation rates in the $|g\rangle$ and $|r\rangle$ states are compared. The general behavior of the dependencies shown in Fig. 3 is similar to that of the curves plotted in Fig. 2. Curve 10 in Fig. 3 and curve 9 in Fig. 2 are identical, because they correspond to the same parameter values. As one can see, the light-pressure force decreases with the growth of $\gamma_g + \gamma_r$ because the coherence relaxation rate γ_{coh} also increases in this case.

Figures 2 and 3 demonstrate the values of the light-pressure force acting on a nanoparticle in the field of counter-propagating bichromatic waves normalized to F_{\max} , the light-pressure force maximum in the field of a monochromatic traveling wave [Eq. (30)]. Since F_{\max} depends on three relaxation constants and α , it is difficult to assess, from those figures, a change in the “bichromatic” force magnitude itself, when the parameters of the atom–field interaction vary. To illustrate this dependence, it is desirable to compare the light-pressure force acting on a nanoparticle in the field of counter-propagating bichromatic waves with either the light-pressure force maximum in the two-level model of an atom in the field of a monochromatic traveling wave, $F_{2\max}$, or the maximum possible light-pressure force in the field of counter-propagating bichromatic waves, F_{bichro} .

In Fig. 4, the α -dependences of the light-pressure force F acting on a nanoparticle are plotted for various values of the relaxation rate $\gamma_g + \gamma_r$ between the states $|g\rangle$ and $|r\rangle$, and the same values of other pa-

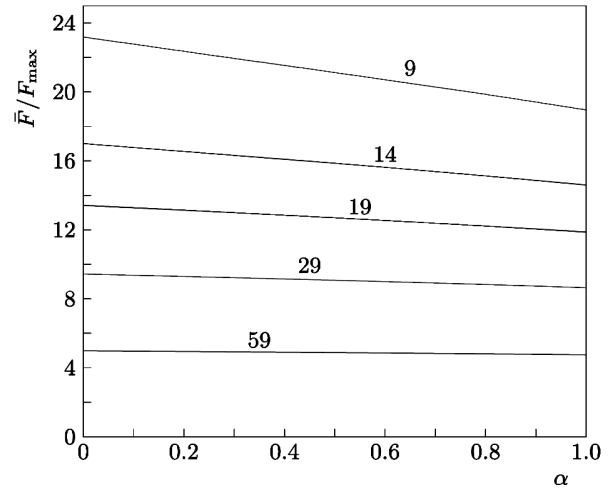


Fig. 2. Dependences of the light-pressure force (in F_{\max} units) acting on a nanoparticle on the parameter α for various coherence relaxation rates $\gamma_{\text{coh}} = \frac{1}{2}(\gamma_g + \gamma_{\text{opt}}) + \gamma_{\text{ph}}$ (indicated in MHz near the curves) and $\gamma_{\text{opt}}/2\pi = 10$ MHz, $\gamma_r/2\pi = 2$ MHz, $\gamma_g/2\pi = 8$ MHz, $\Delta = 0$, $\delta/2\pi = 500$ MHz, $\Omega_0/2\pi = 1225$ MHz, and $\varphi = \pi/4$

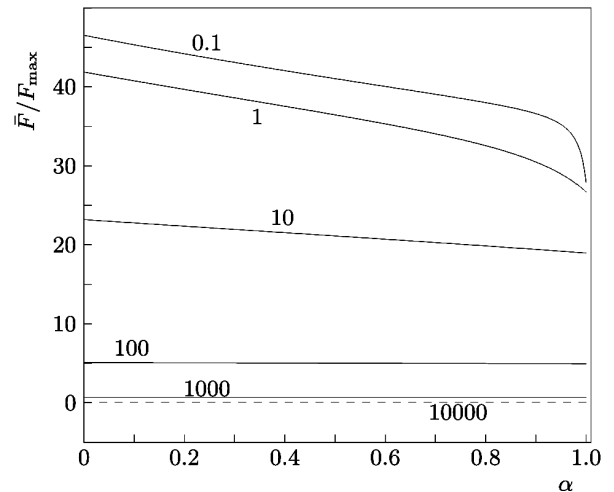


Fig. 3. Dependences of the light-pressure force (in F_{\max} units) acting on a nanoparticle on the parameter α for various relaxation rates $\gamma_g + \gamma_r$ of the states $|g\rangle$ and $|r\rangle$ (the values indicated in MHz near the curves correspond to $\gamma_g = 4\gamma_r$) and $\gamma_{\text{opt}}/2\pi = 10$ MHz, $\gamma_{\text{ph}} = 0$, $\Delta = 0$, $\delta/2\pi = 500$ MHz, $\Omega_0/2\pi = 1225$ MHz, and $\varphi = \pi/4$

rameters of the interaction between the active atom and the field as in Fig. 3. However, this time F is reckoned in the F_{bichro} units. The attention is attracted by a completely different mutual arrangement of the curves with different $\gamma_g + \gamma_r$ values in comparison

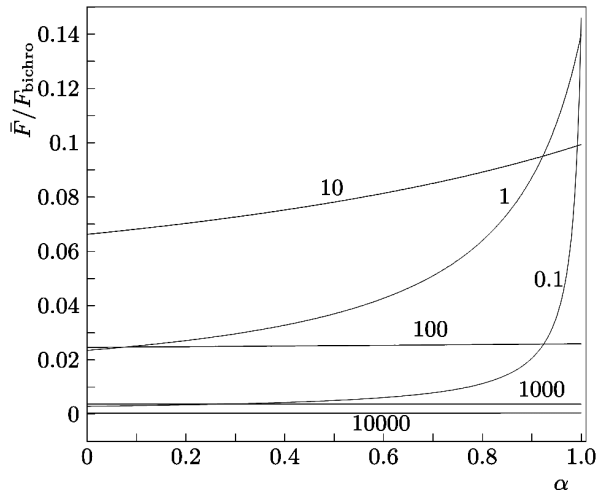


Fig. 4. Dependences of the light-pressure force (in F_{bichro} units) acting on a nanoparticle on the parameter α for various relaxation rates $\gamma_g + \gamma_r$ of the states $|g\rangle$ and $|r\rangle$ (the values indicated in MHz near the curves correspond to $\gamma_g = 4\gamma_r$) and $\gamma_{\text{opt}}/2\pi = 10$ MHz, $\gamma_{\text{ph}} = 0$, $\Delta = 0$, $\delta/2\pi = 500$ MHz, $\Omega_0/2\pi = 1225$ MHz, and $\varphi = \pi/4$

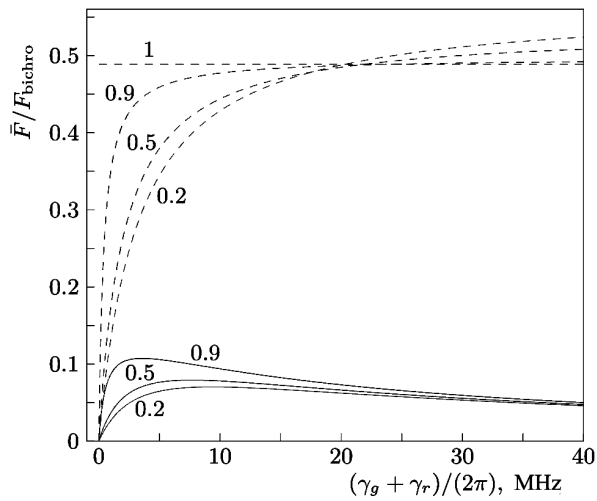


Fig. 5. Dependences of the light-pressure force (in F_{bichro} units) acting on a nanoparticle on the parameter $(\gamma_g + \gamma_r)/(2\pi)$ for various values of the parameter α (indicated near the curves) and $\gamma_{\text{opt}}/2\pi = 10$ MHz, $\Delta = 0$, $\delta/2\pi = 500$ MHz, $\Omega_0/2\pi = 1225$ MHz, $\varphi = \pi/4$, and $\gamma_g = 4\gamma_r$ (solid curves) or $\gamma_g = 0$ (dashed curves)

with that in Fig. 3. According to the latter, the ratio between the pressure force acting on a nanoparticle in the field of counter-propagating bichromatic waves and the maximum pressure force in the traveling-wave field decreases with the growth of $\gamma_g + \gamma_r$, and the

pressure force magnitude itself (Fig. 4 demonstrates that its ratio to F_{bichro}) is small at both very low and very high $\gamma_g + \gamma_r$ values.

The small values of the light-pressure force at low population relaxation rates in the $|g\rangle$ and $|r\rangle$ states may be associated with the accumulation of atoms in the state $|r\rangle$, where they do not interact with the field. A small value of the light-pressure force in the opposite case and at the ratio between the relaxation constants γ_g and γ_r that is indicated in Fig. 4 is explained by the growth of the coherent relaxation rate $\gamma_{\text{coh}} = \frac{1}{2}(\gamma_g + \gamma_{\text{opt}}) + \gamma_{\text{ph}}$. Hence, there must be an optimal value for $\gamma_g + \gamma_r$ that maximizes the light-pressure force. This is possible, if γ_g differs from zero. If $\gamma_g = 0$, the light-pressure force should monotonically increase with the increase of $\gamma_g + \gamma_r = \gamma_r$ and go toward the maximum value obtained in the two-level atomic model.

Indeed, one can see in Fig. 5 that if some non-zero value of α is fixed, and if the sum $\gamma_g + \gamma_r$ grows, the light-pressure force first increases to a certain maximum value and then tends to zero (the light-pressure force is not shown at very large values of $\gamma_g + \gamma_r$). But, if $\gamma_g = 0$, the light-pressure force first grows to the maximum value (for $\alpha = 0.2$, this is 0.5539 at $\gamma_r/2\pi = 220$ MHz) and afterward approaches the values corresponding to the two-level atom (i.e., to the case $\alpha = 1$).

It would appear that the interaction between a three-level atom and the field could be interpreted as a reduction of the role of the third level to a simple population depot and the formation of light-pressure force following the same laws as for the two-level system. In this case, the light-pressure force would be equal to that in the two-level system multiplied by $(n_g + n_e)$, and the dependences shown in Figs. 4 and 5 would be similar to the corresponding $(n_g + n_e)$ -dependences. However, the dependences in Fig. 6 plotted for the same parameters as in Fig. 5 testify that this is not so. It is obvious that the plots in Fig. 5 cannot be obtained from the corresponding plots in Fig. 6 by simply multiplying the ordinates of all curves in Fig. 6 by the same factor.

5.2. Y_2SiO_5 crystal doped with erbium ions

Obvious candidates for “active” atoms in nanoparticles are atoms of rare-earth elements [25], whose ions are used in some crystals to observe electromagneti-

cally induced transparency. If the radiation-induced transitions occur between the states inside the $4f$ shell, those states are weakly perturbed by the field, and all ions interact resonantly with it.

We will consider the light-pressure force acting on nanoparticles using the interaction between counter-propagating light waves and Y_2SiO_5 crystalline nanoparticles with the $^{167}\text{Er}^{3+}$ impurity as an example. Let us briefly consider the spectroscopic characteristics of this crystal, which are given in work [26].

The authors of paper [26] used a Y_2SiO_5 crystal with the added ^{167}Er isotope to observe the electromagnetically induced transparency. At least two Λ -configurations of energy levels suitable for its observation were found. The corresponding transitions approximately correspond to a wavelength of $1.5 \mu\text{m}$. The erbium content in Y_2SiO_5 was 0.005 at.%. The electronic structure of Er^{3+} ions is described by the formula $[\text{Xe}]4f^{11}$. The total moment $\mathbf{J} = \mathbf{L} + \mathbf{S}$ equals $J = 15/2$ in the ground state (the state $^4I_{15/2}$), and $J = 13/2$ in the first excited state (the state $^4I_{13/2}$). Due to the electric field of neighbor atoms, the degeneracy of the $^4I_{15/2}$ state is partially removed, and it becomes split into eight Kramers doublets. The first excited state is split into seven Kramers doublets. The Kramers doublet can be described by the effective electronic spin $S_{\text{eff}} = 1/2$. Two positions of erbium ions in the crystal are possible: an erbium ion has six neighbors in position 1, and seven neighbors in position 2.

The wavelengths of the transitions from the lower Kramers doublet of the ground state $^4I_{15/2}$ into the lower Kramers doublet of the excited state $^4I_{13/2}$ equal $\lambda = 1536 \text{ nm}$ for erbium ions in position 1, and $\lambda = 1538 \text{ nm}$ for erbium ions in position 2. Since the electrons in the $4f$ shell are screened by the filled $5s^2$ and $5p^6$ shells, the frequencies of transitions inside the $4f$ shell are weakly perturbed by the crystalline field.

The spin of the ^{167}Er isotope nucleus is $I = 7/2$. Owing to hyperfine and quadrupole interactions, the Kramers doublets are split into at most $(2S_{\text{eff}} + 1)(2I + 1) = 16$ hyperfine components due to the low symmetry of the crystal even in the absence of the magnetic field. A large number of hyperfine sublevels in the ground and excited states allow the realization of many Λ -schemes of the interaction between an erbium ion and the field. All transitions are allowed, because hyperfine sublevels correspond not to pure quantum states, but to the mixtures of

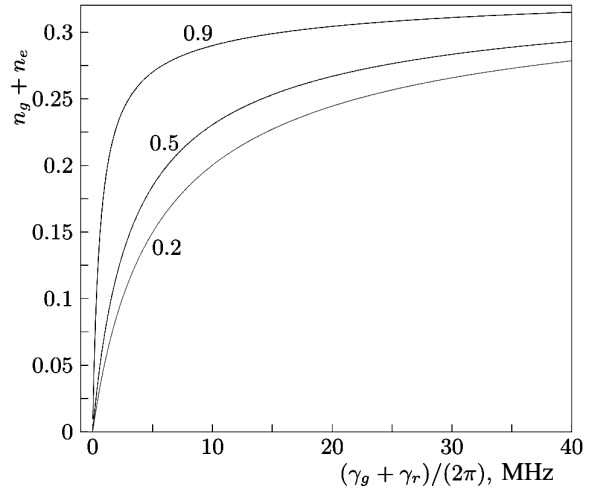


Fig. 6. Dependences of the total population of states $|g\rangle$ and $|e\rangle$ on the parameter $(\gamma_g + \gamma_r)/(2\pi)$ at $\gamma_g = 4\gamma_r$ for various values of the parameter α (indicated near the curves) and $\Delta = 0$, $\delta/2\pi = 500 \text{ MHz}$, $\Omega_0/2\pi = 1225 \text{ MHz}$, $\varphi = \pi/4$, and $\gamma_{\text{opt}}/2\pi = 10 \text{ MHz}$

the states $|I = 7/2, M_I\rangle$, where $M_I = \pm 7/2, \pm 5/2, \pm 3/2, \pm 1/2$ is the projection of the nuclear spin onto the selected axis. An inhomogeneous broadening due to the crystal field non-uniformity has an order of several megahertz. The distance between the ultrafine components of spectral lines amounts to hundreds of MHz. The authors of work [26] managed to determine two relaxation constants: $T_1^{\text{opt}} = 10 \text{ ms}$ and $T_1^{\text{hyp}} = 97 \text{ ms}$. The former determines the lifetime of the ion in the excited state, and the latter the time of the population relaxation between the sublevels of the ground state.

The presented scenario of the atomic interaction with the electromagnetic field makes it possible to formulate a simple model for the interaction between nanoparticles with erbium impurities and the laser radiation field. If the Rabi frequency of laser radiation and the frequency of its amplitude modulation are substantially lower than the frequency difference between the ultrafine structure components, the ion in the crystal environment can be approximately described using the three-level scheme: we have (i) a light-induced transition between two ionic levels (the ground and excited ones); (ii) a transition from the excited state with the relaxation time T_1^{opt} into the ground state and intermediate states that correspond to various components of the hyperfine structure; and (iii) a transition from the intermediate

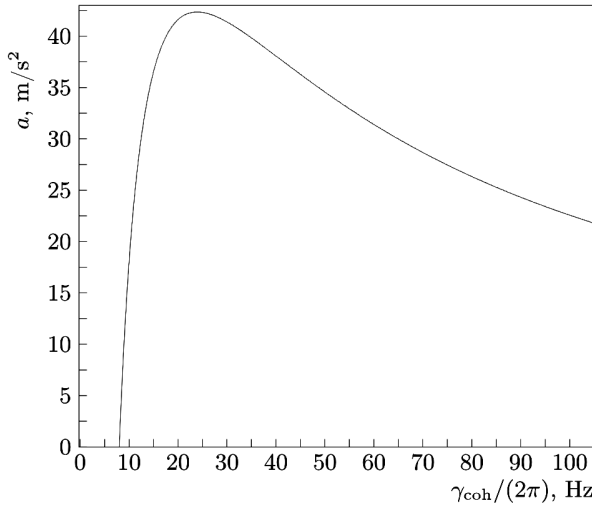


Fig. 7. Dependence of the acceleration of an Y_2SiO_5 nanoparticle doped with $^{167}Er^{3+}$ ions on the coherence relaxation rate $\gamma_{coh} = \frac{1}{2}(\gamma_{opt} + \gamma_g) + \gamma_{ph}$ for $\gamma_{opt}/2\pi = 16$ Hz, $\gamma_{ph} = 0$, $(\gamma_g + \gamma_r)/\gamma_r = 100$, $\Delta = 0$, $\delta/2\pi = 204$ MHz, $\Omega_0/2\pi = 500$ MHz, and $\varphi = \pi/4$

state into the ground state owing to the relaxation (the characteristic time T_1^{hyp}).

5.3. Selection of laser radiation parameters and calculation of light-pressure force acting on a nanoparticle in $^{167}Er^{3+}$ -doped Y_2SiO_5

The characteristic energy difference between the hyperfine state levels of an erbium-167 ion in the Y_2SiO_5 crystal corresponds to hundreds of megahertz. In particular, for the lowest two levels, it is equal to 740 MHz [26]. The Rabi frequency of the light waves acting on the nanoparticle must be considerably lower than this value, e.g., 500 MHz. Let us estimate the intensity of laser radiation corresponding to this frequency.

We assume that the lifetime of the ion in the excited state is $T_1^{opt} = 10$ ms, which gives $\gamma_{opt} = 10^2$ s $^{-1}$ (≈ 16 Hz). For a monochromatic traveling wave with the intensity E_0 and the dipole electric transition in an atom with the projection of the matrix element of the dipole moment d_{ge} between the states $|g\rangle$ and $|e\rangle$ of the ion onto the polarization vector ϵ , the Rabi frequency Ω equals [27]

$$|\Omega[\text{rad/nsec}]| = 0.22068 \frac{|d_{21} \epsilon|}{ea_0} \sqrt{I [\text{W/cm}^2]}. \quad (55)$$

Here, I is the intensity of laser radiation.

The dipole moment is related to the Einstein coefficient A_{12} (in our case, this is γ_{opt}) via the relation [27] (in SGSE units)

$$|d_{12}|^2 = \frac{3 \hbar}{4 k^3} \varpi_1 A_{12}, \quad (56)$$

where ϖ_1 is the statistical weight of the state $|g\rangle$, which, in our case, is of an order of 10^2 (this is the total number of the levels of fine and ultrafine structure α^{-1} , onto which transitions from the excited state are possible). From Eq. (56), we get the estimate

$$\frac{|d_{12}|}{ea_0} = \frac{\sqrt{3}}{2ea_0k^2} \sqrt{\hbar k \varpi_1 A_{12}}, \quad (57)$$

which gives $|d_{12}|/(ea_0) = 0.129$ for $A = 100$ s $^{-1}$ and $\lambda = 1.5$ μm . At an intensity of an order of 100 W/cm 2 , Eq. (55) yields $\Omega/2\pi = 45.3$ MHz. The Rabi frequency of 500 MHz corresponds to the laser radiation intensity of about 12 kW/cm 2 .

5.4. Acceleration of an $^{167}Er^{3+}$ -doped Y_2SiO_5 nanoparticle under the action of light-pressure force

In order to calculate the light-pressure force, besides the selected parameters, it is also necessary to know the coherence relaxation rate. According to the results of work [28], the characteristic coherence lifetime T_{coh} ranges from 1 μs to 20 ms depending on the temperature, the applied magnetic field, and the concentration of erbium ions in the crystal. This coherence time interval corresponds to the interval of coherence relaxation rates $\gamma_{coh}/(2\pi)$ from 8 Hz (it corresponds to $\frac{1}{2}\gamma_{opt}$) to 160 kHz.

Let us calculate the acceleration of a nanoparticle, if the mass concentration of erbium equals 1%. From the dependence of the nanoparticle acceleration on the coherence relaxation rate shown in Fig. 7, one can see that, for the selected calculation parameters, the maximum expected acceleration is 42 m/s 2 at $\gamma_{coh}/2\pi = 24$ Hz. The value of γ_r required for the calculation was chosen from the total number of about 100 populated levels of hyperfine structure (seven Kramers doublets, with each of them being split into 16 components). Assuming all of them to be characterized by approximately the same parameters of the interaction with the field, one of them to be working, and the others to be described by the state

$|r\rangle$, we come to the conclusion that $\alpha = 0.01$ and $\gamma_g = 100\gamma_r$. The last estimate follows from the expressions for the equilibrium populations of the states $|g\rangle$ and $|r\rangle$ [Eq. (15)]. Those requirements are satisfied by $\gamma_g/2\pi = 16$ Hz and $\gamma_r/2\pi = 0.16$ Hz. We also assume that there is no additional increase of the relaxation rate due to fluctuations ($\gamma_{ph} = 0$). The fact that there is no acceleration of the nanoparticle at $\gamma_{coh}/2\pi = 8$ Hz is not surprising, because this value corresponds to $\gamma_g = \gamma_r = 0$, which brings about the zero populations of the states $|g\rangle$ and $|e\rangle$ due to the optical pumping into the $|r\rangle$ state.

From the plotted dependence of the nanoparticle acceleration on the coherence relaxation rate, we can see that the expected acceleration of nanoparticles is rather low as compared to the acceleration of atoms in the field of bichromatic waves. It is quite possible that nanoparticles with an admixture of other “active” atoms for which the value of α is higher may move with a much higher acceleration.

5.5. Negatively charged silicon color centers at vacancies in diamond

Another candidate for “active” atoms can be the SiV and GeV color centers that arise owing to the localization of silicon or germanium atoms at the vacancies of the diamond crystal [29, 30]. The spectral characteristics of color centers are determined by the energy levels of an electron captured at defects in the crystalline lattice. The required optical properties (a narrow inhomogeneous width and a rather narrow spectral line) arise due to the inversion symmetry [31], which results in the disappearance of permanent electric dipole moments in the orbital Si states and drastically reduces their response to charge fluctuations in the local medium.

Let us estimate the light-pressure force acting on diamond nanoparticles containing SiV color centers. Owing to the spin-orbit interaction, each of the ground and excited states of SiV is split into two ones. As a result, the transition of an excited atom into two states becomes possible, which forms a three-level scheme of the silicon interaction with laser radiation. The radiation wavelength is $\lambda = 737$ nm, and the spontaneous radiation rate is $\gamma_{opt}/2\pi = 94$ MHz [29]. The non-uniform linewidth is approximately three times as large as $\gamma_{opt}/2\pi$. To estimate the coherence relaxation rate, we use the expression $\gamma_{coh} =$

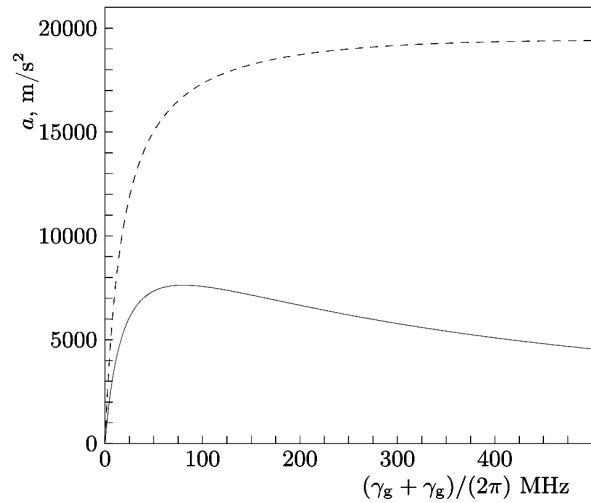


Fig. 8. Dependences of the nanoparticle acceleration on the parameter $(\gamma_g + \gamma_r)/(2\pi)$ for $\gamma_g = \gamma_r$ (solid curve) and $\gamma_g = 0$ (dashed curve), and $\Delta = 0$, $\delta/2\pi = 500$ MHz, $\Omega_0/2\pi = 1225$ MHz, $\varphi = \pi/4$, $\gamma_{ph} = 0$ MHz, and $\alpha = 0.5$. The mass fraction of silicon is 0.01%

$= \frac{1}{2}(\gamma_{opt} + \gamma_g) + \gamma_{ph}$, but neglect the fluctuation term γ_{ph} in it. The Rabi frequency has to be much higher than $\gamma_{opt} = 94$ MHz. Let $\Omega_0/2\pi = 1225$ MHz and $\delta/2\pi = 500$ MHz. Using Eqs. (55) and (57), we find that such a value for the Rabi frequency is reached at a radiation intensity of 5.2 W/cm² due to a rather wide radiation line and, accordingly, a large value of the transition dipole moment ($d_{12} = 15.3ea_0$).

Let us assume that, after the spontaneous emission, silicon atoms can turn out with the same probability ($\alpha = 0.5$) on either of the lower levels. Concerning the relaxation constants γ_g and γ_r , let us consider two cases: (i) when, in the field absence, due to the relaxation between the states $|g\rangle$ and $|r\rangle$, their populations get equalized, i.e., $\gamma_g = \gamma_r$, and (ii) when $\gamma_g = 0$ so that, in the field absence, all silicon atoms are in the state $|g\rangle$. Owing to the lack of data on the relaxation rate, let us calculate the dependence of the light-pressure force acting on a nanoparticle on the quantity $\gamma_g + \gamma_r$. The results of calculations of the dependence of the nanoparticle acceleration obtained for the indicated parameters are shown in Fig. 8. If relaxation is slow as is expected, the nanoparticle acceleration is low, because a substantial fraction of the atoms are in the $|r\rangle$ state in this case and do not interact with the laser radiation.

If the silicon content in diamond equals 0.01 wt.%, the diamond mass per silicon atom amounts to

4.65×10^{-23} g, which corresponds to a volume of 133 nm^3 . For the expected acceleration of 5000 m/s^2 , the light-pressure force arising due to the interaction of a silicon atom with the laser radiation field equals 2.3 fN . The diameter of a spherical nanoparticle containing 1000 silicon atoms with the indicated mass concentration equals 63 nm .

According to work [32], the light-pressure force exerted by a monochromatic wave of intensity I on a dielectric sphere of radius $a \ll \lambda$ equals

$$F = \frac{8}{3} \pi \frac{n_2}{c} (ka)^4 a^2 \left(\frac{n_1^2 - n_2^2}{n_1^2 + 2n_2^2} \right) I, \quad (58)$$

where n_1 and n_2 are the refractive indices of the nanoparticle and the medium, respectively. For diamond, $n_1 = 2.4$. Let nanoparticles with the diameter $2a = 63 \text{ nm}$ be in air ($n_2 = 1$) in the radiation field with an intensity of 5.2 W/cm^2 . In this case, from Eq. (58), we have $F = 4.6 \times 10^{-6} \text{ fN}$, which is six orders of magnitude less than the given above estimate of the light-pressure force arising due to the interaction of SiV color centers with the laser field radiation. Such a large difference between the forces of light pressure on nanoparticles partially results from the small nanoparticle radius. Really, it follows from Eq. (58) that the acceleration of a small nanoparticle associated with its dielectric properties is proportional to the cube of nanoparticle radius, whereas the acceleration acquired due to the resonant light pressure on “active” atoms does not depend on the nanoparticle size, at least as far as the nanoparticle contains considerably more than one atom.

6. Conclusions

The method for calculating the light-pressure force acting on atoms and nanoparticles containing an admixture of “active” atoms in the field of counter-propagating bichromatic light waves has been described and developed for the case where the interaction of atoms with the field can be described in the framework of the three-level scheme. The calculations are based on the solution to three-term recurrence relations, which were used earlier by the authors while analyzing the interaction of two-level atoms with the laser radiation field.

The presence of a third level, which the atoms can get to in the course of the relaxation followed by the relaxation to the ground state, decreases the light-pressure force. It is shown that this decrease is not

directly related to a change in the populations of two working levels, because the dependences of the light-pressure force and the total population of the working levels on the problem parameters are different.

The force of light pressure on Y_2SiO_5 nanoparticles doped with $^{167}\text{Er}^{3+}$ ions is calculated. The acceleration value of about 40 m/s^2 , which is found for nanoparticles, is sufficient to register the light-pressure force arising in the field of counter-propagating bichromatic waves, although it is several orders of magnitude less than the acceleration of a two-level atom under the same conditions.

According to the results of our calculations, color centers are more promising than lanthanides for their application as “active” atoms in diamond. It is found that the nanoparticle acceleration can reach a value of about 5000 m/s^2 for a silicon mass concentration in diamond at a level of 0.01% . This value is two orders of magnitude higher than the expected acceleration of nanoparticles from Y_2SiO_5 doped with $^{167}\text{Er}^{3+}$ ions to an order of magnitude higher concentration of rare earth ions.

The concept of using “active” atoms to enhance the light pressure on nanoparticles allows the light-pressure force acting on small, much smaller than the radiation wavelength, nanoparticles to be increased by several orders of magnitude.

Besides performing the calculations of light-pressure forces acting on nanoparticles with “active” atoms, a force calculation method is developed and can also be used in the case where the interaction of a free atom with the field cannot be reduced to the two-level scheme.

The work was carried out in the framework of the Target Program of Basic Research of the National Academy of Sciences of Ukraine “Promising fundamental research and innovative developments of nanomaterials and nanotechnologies for the needs of industry, health care, and agriculture”.

1. J.L. Killian, F. Ye, M.D. Wang. Optical tweezers: A force to be reckoned with. *Cell* **175**, 1445 (2018).
2. P. Polimeno, A. Magazzú, M.A. Iati, F. Patti, R. Saija, C.D. Esposti Boschi, M.G. Donato, P.G. Gucciardi, P.H. Jones, G. Volpe, *et al.* Optical tweezers and their applications. *J. Quantitative Spectroscopy and Radiative Transfer* **218**, 131 (2018).
3. S.T. Müller, D.V. Magalhães, R.F. Alves, V.S. Bagnato. Compact frequency standard based on an intracavity sam-

- ple of cold cesium atoms. *J. Opt. Soc. Am. B* **28**, 2592 (2011).
4. V. Shah, R. Lutwak, R. Stoner, M. Mescher. A compact and low-power cold atom clock. In: *2012 IEEE International Frequency Control Symposium Proceedings* (2012), p. 1.
 5. F.P. dos Santos, S. Bonvalot. *Cold-Atom Absolute Gravimetry* (Springer International Publishing, 2016).
 6. V.G. Minogin, V.S. Letokhov. *Laser Light Pressure on Atoms* (Gordon and Breach, 1987).
 7. H.J. Metcalf, P. van der Stratten. *Laser Cooling and Trapping* (Springer-Verlag, 1999).
 8. A.P. Kazantsev. Acceleration of atoms by light. *Zh. Eksp. Teor. Fiz.* **66**, 1599 (1974) (in Russian).
 9. V.S. Voitsekhovich, M.V. Danileiko, A.M. Negriiko, V.I. Romanenko, L.P. Yatsenko. Light pressure on atoms in counterpropagating amplitude-modulated waves. *Sov. Phys. Tech. Phys.* **33**, 690 (1988).
 10. V.S. Voitsekhovich, M.V. Danileiko, A.N. Negriiko, V.I. Romanenko, L.P. Yatsenko. Observation of a stimulated radiation pressure of amplitude-modulated light on atoms. *JETP Lett.* **49**, 161 (1989).
 11. J. Söding, R. Grimm, Y. Ovchinnikov, P. Bouyer, C. Salomon. Short-Distance atomic beam deceleration with a stimulated light force. *Phys. Rev. Lett.* **78**, 1420 (1997).
 12. L. Yatsenko, H. Metcalf. Dressed-atom description of the bichromatic force. *Phys. Rev. A* **70**, 063402 (2004).
 13. A.M. Negriiko, V.I. Romanenko, L.P. Yatsenko. *Dynamics of Atoms and Molecules in Coherent Laser Fields* (Naukova dumka, 2008) (in Russian).
 14. H. Metcalf. Strong optical forces on atoms in multifrequency light. *Rev. Mod. Phys.* **89**, 041001 (2017).
 15. V.I. Romanenko, L.P. Yatsenko. Stimulated radiation pressure acting on an atom nonadiabatically interacting with the field of counterpropagating frequency-modulated waves. *JETP Lett.* **86**, 756 (2007).
 16. V. Romanenko, B. Shore, L. Yatsenko. Forces exerted on atoms by stochastic laser fields. *Optics Communications* **268**, 121 (2006) ISSN 0030- 4018.
 17. V.I. Romanenko, L.P. Yatsenko. Theory of onedimensional trapping of atoms by counterpropagating short pulse trains. *J. Phys. B: Atomic, Molecular and Optical Phys.* **44**, 115305 (2011).
 18. V.I. Romanenko, Y.G. Udovitskaya, A.V. Romanenko, L.P. Yatsenko. Cooling and trapping of atoms and molecules by counterpropagating pulse trains. *Phys. Rev. A* **90**, 053421 (2014).
 19. V.I. Romanenko, O.V. Romanenko, L.P. Yatsenko. An optical trap for atoms on the basis of counter-propagating bichromatic light waves. *Ukr. J. Phys.* **61**, 309 (2016).
 20. V.I. Romanenko, N.V. Kornilovska. Atoms in the counter-propagating frequency-modulated waves: splitting, cooling, confinement. *Eur. Phys. J. D* **71**, 229 (2017).
 21. M. Kerker. *The Scattering of Light and Other Electromagnetic Radiation* (Academic press, 1969).
 22. L. Podlecki, R. Glover, J. Martin, T. Bastin. Radiation pressure on a two-level atom: An exact analytical approach. *JOSA B* **35**, 127 (2018).
 23. L. Podlecki, J. Martin, T. Bastin. Radiation pressure on single atoms: Generalization of an exact analytical approach to multilevel atoms. *J. Opt. Soc. Am. B* **38**, 3244 (2021).
 24. V.I. Romanenko, L.P. Yatsenko. Evolution of the velocity distribution of atoms under the action of the bichromatic force. *Phys. Rev. A* **103**, 043104 (2021).
 25. R.L. Cone, C.W. Thiel, Y. Sun, T. Böttger, R.M. Macfarlane. Rare-earth-doped materials with application to optical signal processing, quantum information science, and medical imaging technology. *Proc. SPIE* **8272**, 82720E (2012).
 26. E. Baldit, K. Bencheikh, P. Monnier, S. Briauudeau, J.A. Levenson, V. Crozatier, I. Lorgeré, F. Bretenaker, J.L. Le Gouët, O. Guillot-Noël *et al.* Identification of Λ -like systems in $\text{Er}^{3+}:\text{Y}_2\text{SiO}_5$ and observation of electromagnetically induced transparency. *Phys. Rev. B* **81**, 144303 (2010).
 27. B. Shore. *The Theory of Coherent Atomic Excitation* (Wiley, 1990), Vol. 1.
 28. T. Böttger, C.W. Thiel, Y. Sun, R.L. Cone. Optical decoherence and spectral diffusion at $1.5 \mu\text{m}$ in $\text{Er}^{3+}:\text{Y}_2\text{SiO}_5$ versus magnetic field, temperature, and Er^{3+} concentration. *Phys. Rev. B* **73**, 075101 (2006).
 29. R.E. Evans, A. Sipahigil, D.D. Sukachev, A.S. Zibrov, M.D. Lukin. Narrow-linewidth homogeneous optical emitters in diamond nanostructures via silicon ion implantation. *Phys. Rev. Applied* **5**, 044010 (2016).
 30. M.K. Bhaskar, D.D. Sukachev, A. Sipahigil, R.E. Evans, M.J. Burek, C.T. Nguyen, L.J. Rogers, P. Siyushev, M.H. Metsch, H. Park *et al.* Quantum nonlinear optics with a germanium-vacancy color center in a nanoscale diamond waveguide. *Phys. Rev. Lett.* **118**, 223603 (2017).
 31. C. Hepp, T. Müller, V. Waselowski, J.N. Becker, B. Pingault, H. Sternschulte, D. Steinmüller-Nethl, A. Gali, J.R. Maze, M. Atatüre *et al.* Electronic structure of the silicon vacancy color center in diamond. *Phys. Rev. Lett.* **112**, 036405 (2014).
 32. Y. Harada, T. Asakura. Radiation forces on a dielectric sphere in the Rayleigh scattering regime. *Optics Communications* **124**, 529 (1996).

Received 10.12.22.

Translated from Ukrainian by O.I. Voitenko

В.І. Романенко, Н.В. Корніловська, Л.П. Яценко

СВІТЛОВИЙ ТИСК НА НАНОЧАСТИНКИ
У ПОЛІ ЗУСТРІЧНИХ БІХРОМАТИЧНИХ ХВИЛЬ
З ДОДАТКОВИМ КАНАЛОМ РЕЛАКСАЦІЇ
НАСЕЛЕНОСТІ ЗБУДЖЕНОГО СТАНУ

Розглянуто силу світлового тиску на наночастинки, що містять домішки атомів або центри забарвлення, які резонансно взаємодіють з полем. Найявне кристалічне оточення у загальному випадку унеможливило формування дворівневої

схеми взаємодії атома або центра забарвлення з полем завдяки зняттю заборони на частину переходів зі спонтанним випромінюванням. У результаті частина атомів перебуває у станах, які не взаємодіють з полем лазерного випромінювання, але які з часом релаксують до основного стану. Побудовано теорію, яка дозволяє розрахувати силу світлового тиску на атоми чи центр забарвлення (і, відповідно, на наночастинку, в якій вони перебувають) у залежності від параметрів їхньої взаємодії з полем та параметрів релаксації збудженого стану і проміжних станів. Для вивчення впливу різних факторів на силу світлового тиску розрахун-

ки проведені для модельної сукупності параметрів, а також для параметрів, які визначають взаємодію тризарядних іонів ербію у допованих ним кристалах Y_2SiO_5 та центрів забарвлення, що виникають завдяки розташуванню атомів кремнію в дефектах кристала алмазу. Як виявилось, завдяки центрам забарвлення можна на кілька порядків підняти силу тиску світла на малі, значно менші за довжину хвилі, наночастинки.

Ключові слова: атоми, наночастинки, лазерне випромінювання, світловий тиск.